25th ABCM International Congress of Mechanical Engineering
October 20-25, 2019, Uberlândia, MG, Brazil

COB-2019-0901
DRIVETRAIN RESISTANCE MODELING APPLIED TO SMALL WIND TURBINES

Ruan de Souza Ribeiro[1]
Erick Oliveira do Nascimento[2]
Davi Cavalcante de Oliveira[3]
Marilza dos Santos Viana[4]
Jerson Rogério Pinheiro Vaz[5]
Federal University of Pará, Graduate Program in Mechanical Engineering. Augusto Corrêa Avenue, 1, Guamá, 66075-110. Belém, PA, Brazil
[1]ruan.ribeiro@tucurui.ufpa.br, [2]oliveira94n@gmail.com, [3]daviufpappgem@gmail.com, [4]marilza.viana@ymail.com, [5]jerson@ufpa.br

Abstract. *The friction presents several nonlinear characteristics becoming difficult its modeling. Also, its dynamic characteristics need to be planned or adequately compensated to reduce friction effects. This work presents a study of the starting performance of a horizontal-axis small wind turbine drivetrain, considering the friction phenomena of bearings typically used in wind systems. A theoretical mathematical analysis was carried out, and a new dynamic model was developed in order to consider the effects of static and dynamic friction on the behavior of wind turbines. The mathematical approach was compared using experimental data available in the literature.*

Keywords: *friction, wind turbine, drivetrain, dynamic model*

1. INTRODUCTION

Small wind turbines are those which have their rotor diameter ranging from 3 to 10 m, and having a power capacity of 1.4–20 kW (Tummala et al., 2016). Also, the International Electrotechnical Commission standard for this scale (IEC 61400-2) defines them as having a rotor swept area smaller than or equal to 200 m², generating electricity at a voltage below to 1000 V a.c. or 1500 V d.c. for both on-grid and off-grid applications. Yet, those turbines work at low wind speed.

According to Wood (2011), there are at least three reason to be interested by performance this characteristic of wind. The first one, many small turbines are located close to the load they supply and this may not be a good wind site. Secondly, few small turbines have pitch mechanism, so that a blade designed for optimal power extraction at a high tip speed ratio, will present high angles of attack when it is stationary. Lastly, turbines start only when the aerodynamic torque generated on the stationary blades exceeds the resistive torque in the generator and drivetrain.

Usually, small wind turbines do not have pitch adjustment of the blades, making starting at low wind speed a serious challenge magnified by the drivetrain resistance caused by bearing friction or generator cogging torque (Vaz et al., 2018). The resistive torque is much less than the rated generator torque so drivetrain resistance is safely ignored once power production commences but must be considered when the rotor torque is low. This situation occurs during starting and when the turbine approaches the runaway condition of no output load.

Ebert and Wood (1997), considered the characteristics of the starting performance of a small horizontal-axis wind turbine in the context of a simple, quasi-steady analysis of the complex aerodynamics dominated by unsteadiness, high angles of attack, and low Reynolds number. The bearings, gearboxes and generators of small turbines often have a significant resistive torque that must be overcome aerodynamically before the blades will start turning. Furthermore, pitch control is rarely used on small wind turbines because of cost (Wood, 2011).

Thereby, this work has as the principal goal been developing a mathematical modeling using Generalized Maxwell-Slip (GMS) friction model to study the starting performance of a horizontal-axis small wind turbine drivetrain, considering the friction phenomena of bearings typically used in wind systems. Recently, Stammler et al. (2018), studied different operating conditions to evaluate the influence of pitch bearings in a 3 MW class turbine, their work shows good agreement and Vaz et al. (2018), observed that to assess starting behavior, it is necessary to include the effect of static friction torque in the turbine design, as it is extremely necessary to estimate starting wind velocity. Generally, static resistance is often significantly higher than the dynamic one. This difference is usually attributed to the Stribeck effect, which accounts resistive torque when the turbine is under eminent moving. This study is compared with some experimental results already tested in literature to analyze the behavior of the model in question.

2. DYNAMIC MODEL

The wind turbine studied consists of an aerodynamic rotor with mass-moment of inertial J_T connected by a shaft to the drivetrain supported by two deep-groove ball bearings which transfer reaction loads to the main frame of the turbine, as illustrated in Fig. 1, that are part of a magnetic brake. The balance of the drivetrain has an inertial of J_S.

The wind turbine studied consists of an aerodynamic rotor with mass-moment of inertial J_T connected by a shaft to the drivetrain supported by two deep-groove ball bearings which transfer reaction loads to the main frame of the turbine, as illustrated in Fig. 1, that are part of a magnetic brake. The balance of the drivetrain has an inertial of J_S.

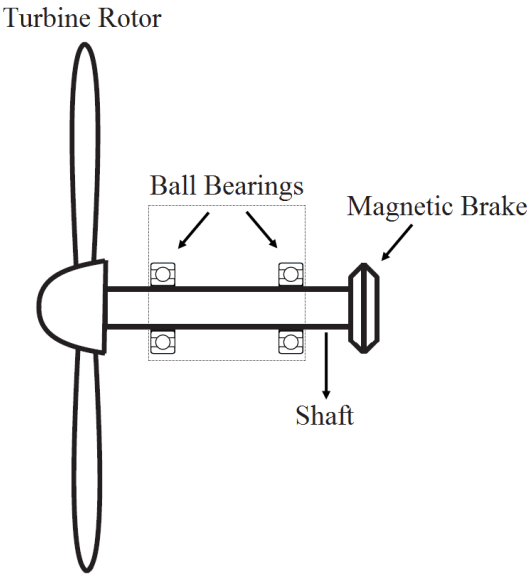

Figure 1. Illustration of the system of a small wind turbine.

Equation (1) shows the torque balance on the turbine:

$$J_T + J_S \frac{d\omega_T}{dt} = T_T - T_D \tag{1}$$

where ω_T is the turbine angular speed, T_T the rotor turbine torque and T_D the resistive torque of bearings. The blades start only when the rotor turbine torque generated is greater than the resistive torque in the bearings.

The bearing friction is analyzed for two cases: dynamic and static. Palmgren (1959), separated the frictional torque into a load-dependent component (T_L) and a load-independent component (T_V) which is influenced by the lubricant type, the amount of the lubricant employed and bearing speed. T_L and T_V are given by empirical formulas. The Eq. (2) presents the mathematical formulation for the Palmgren model.

$$T_D = T_L + T_V \tag{2}$$

In order to compensate the friction effects in bearings, the Eq. (2) needs to be modified and one more term is added becomes Eq. (3):

$$T_D = T_L + T_V + T_F \tag{3}$$

where T_F is the dissipative torque during the powertrain starting. In this work, the Generalized Maxwell-Slip (GMS) model was used.

2.1 Generalized Maxwell-slip friction model

Lampaert et al. (2003), developed a generic friction model which simulates the contact physics at asperity level. The Generalized Maxwell-Slip (GMS) friction model is based explicitly on three friction properties. First, the Stribeck curve for constant velocities. Second, the hysteresis function with non-local memory in the presliding regime, and third the frictional memory in the sliding regime. The developed model is a parallel connection of different single state friction

models, all having the same input namely the velocity (v). The friction force is given as the summation of the outputs of the N elementary state models plus an extra viscous term, if viscous friction is present at the interface, as shown in Eq. (4):

$$F_F(t) = \sum_{i=1}^{N} F_i(t) + \sigma_2 v(t). \tag{4}$$

The dynamic behavior of each elementary model can be written if the elementary model is sticking by the Eq. (5) or if it's slipping is given by Eq. (6):

$$\frac{dF_i}{dt} = k_i v \tag{5}$$

$$\frac{dF_i}{dt} = \text{sgn}(v) C \left(1 - \frac{F_i}{S(v)} \right) \tag{6}$$

where k_i is asperity stiffness, C is an attraction parameter and S is the Stribeck curve for constant steady state velocities. The Stribeck's curve is calculated by Eq. (7):

$$S(v) = F_{St} \exp\left[-\left(\frac{v}{v_{St}} \right)^i \right] + \sigma v \tag{7}$$

where F_{St} is the Stribeck friction force, it depends on the static frictional force (F_S) and the Coulomb frictional force (F_C), v_{St} is the Stribeck velocity, i is the Stribeck exponent and σ is the viscous friction coefficient.

Writing the friction force F_F as a function of the friction torque T_F, the friction force was multiplied by the bearing pitch radius d_m. The shaft linear velocity was also written as a function of the shaft rotational speed (n).

2.2 Verification of the friction model

A verification, in order to evaluate GMS accuracy is performed, using the parameters available in Tab. 1.

Table 1. Parameters used in the GMS model.

PARAMETERS	VALUES	UNITS
C	12	N/s
F_S	11.6	N
F_C	0.0	N
v_{St}	0.08	mm/s
i	0.53	-

The velocity dependent on time is required, and it is calculated through Eq. (8):

$$v = \cos\left(\frac{\pi}{2} t \right) + 1 \tag{8}$$

where t is the time in seconds. Eq. (7) was solved without considering the viscous friction coefficient.

The Fig. 2 shows the Stribeck curve compared with experimental results obtained by Lampaert et al. (2003), and the friction force as a function of the velocity.

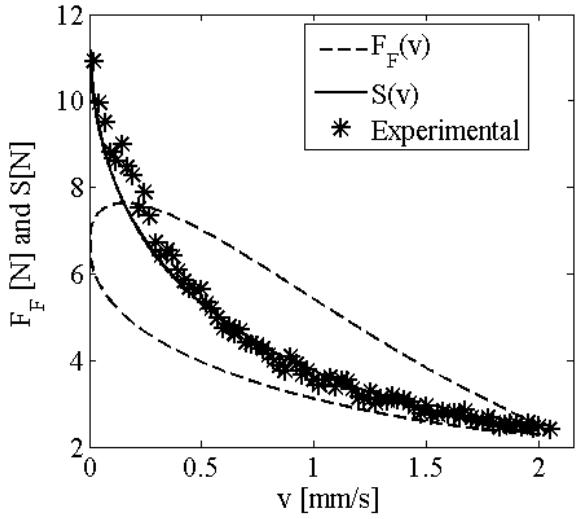

Figure 2. Stribeck curve and the friction force as a function of the velocity.

Note that Stribeck curve presents good agreement compared with experimental data, demonstrating the GMS accuracy. The model shows higher friction force when the velocity decreases presenting good physical behavior, as at low velocity the static friction has relevant influence on the starting.

2.3 Drivetrain starting analysis

To assess the theoretical mathematical developed, the Eq. (3) was solve and the results are compared with experimental data obtained by Vaz et al. (2018), using a torque sensor coupled to a magnetic brake. The calculations are done whereas only radial reactions on the bearings. The parameters available in Tab. 2 were employed to solve the Eqs. (5) and (6).

Table 2. Parameters used.

PARAMETERS	VALUES	UNITS
d_m	31	mm
k	1 x 10^{-6}	N/mm
C	50	N/s
T_S	40.5	Nmm
T_C	0.8	Nmm
n_{St}	0.0037	RPM
i	1.068	-
σ	15.0954	Ns/mm

Therefore, using the Eq. (3), the new expression for the resistive torque yields the Eqs. (9) and (10):

$$T_D = T_L + T_V + T_F + 0.5C_{MPB} \tag{9}$$

$$T_D = 0.0083 + 0.0967n^{0.67} + T_F + 1.378 \tag{10}$$

where C_{MPB} is an additional term, for the constant drag torque of the torque sensor MPB70, whose value is 2.756, and T_F is calculated thought Eqs. (5) and (6) for a Stribeck curve, given by Eq. (11):

$$S(n) = 40.5\exp\left[-\left(\frac{n}{0.0037}\right)^{1.068}\right] + 15.0954n \tag{11}$$

the rotational speed (n) needs to be parametrized by the time. The function shown in Eq. (12) was used:

$$n(t) = \ln(t+1) \tag{12}$$

and then the resistive torque was calculated.

3. RESULTS

Figure 3 shows a comparison between experimental data obtained by Vaz et al. (2018), and the methodology developed in this work. It is worth noting that the accordance is rather accurate using both GMS and Stribeck curve only. This occurs because GMS model is a generalization of Stribeck approximation. The range of angular velocity over which the resistive torque was found for the wind turbine starting experiments is probably too small to show the increase in resistance with increasing *n*. Further, within that range, C_{MPB} is significantly larger than the bearing resistance so any change in the latter *n* is not obvious.

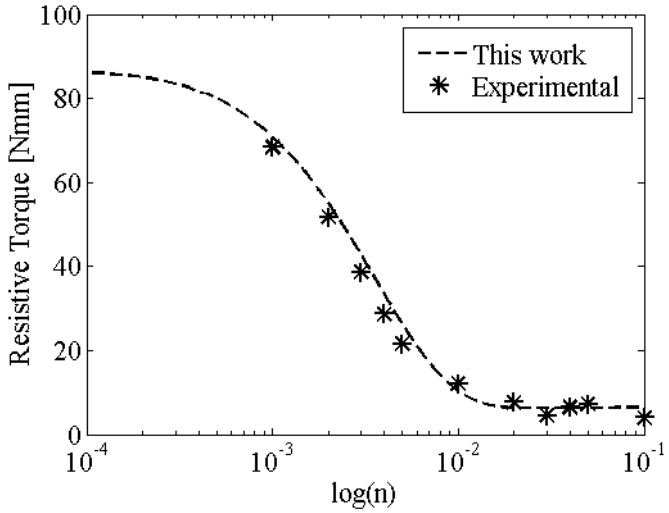

Figure 3. Resistive torque as a function of the rotational speed.

The value of attraction parameter C = 50 was determined using the trial and error method. Perhaps this parameter can have a great influence on the result. Fig. 4 shows different curves for two values of C.

Also, Fig. 4 shows that when the parameter C is augmented, the curve converges to Stribeck approximation. In the GMS friction model this parameter is introduced to directly account for frictional lag dynamics, the attraction parameter is estimated using least-squares techniques measuring the velocity, the friction force and the estimated Stribeck curve $S(v)$ in the sliding regime.

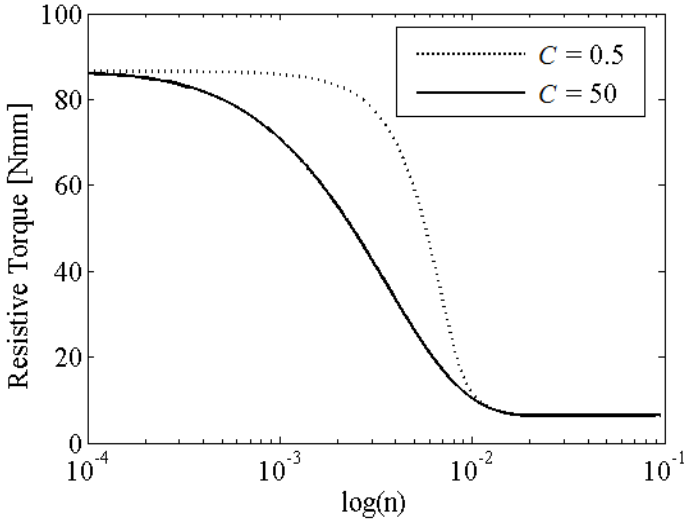

Figure 4. Results for different attraction parameters.

4. CONCLUSIONS

This work presents a novel application for the GMS model during starting of small turbine drivetrain. This theme is important because starting behavior of small turbines is still challenge in the literature, since friction torque is always big during starting for small turbines. The resistive torque was calculated using Palmgren (1959) associated with GMS. This approach presents a very good agreement when compared with experiments. This occurs mainly because GMS contains the Stribeck approximation, which is indeed useful during drivetrain starting. Even though the present approach has good performance with experimental data, the main limitation of this study is that the attraction parameter, *C*, needs to be further investigated, as it is fundamental to ensure convergence in the present model.

5. ACKNOWLEDGEMENTS

The authors would like to thank the CNPq, the Coordenação de Aperfeiçoamento de Pessoal de Nível Superior PROCAD/CAPES (Agreement: 88881.200549/2018-01) and PROPESP/PPGEM/UFPA for financial support.

6. REFERENCES

Ebert, P.R. and Wood, D.H. "Observations of the starting behavior of small horizontal-axis wind turbine". *Renewable Energy*, Vol. 12, No. 3, pp. 245-257.

Hau, E., 2008. *Wind turbines: fundamentals, technologies, application, economics*. Springer, Berlim, 2nd edition.

International Electrotechnical Commission, IEC 61400-2:2014. *Wind turbines – Part 2: design requerements for small wind turbines.* International Standard.

Lampaert, V., Al-Bender, F. and Swevers, J., 2003. "A Generalized Maxwell-Slip Friction Model Appropriate for Control Purposes". In *Proceedings of the 2003 International Conference Physics and Control.* Saint Petersburg, Russia.

Palmgren, A., 1959 *Ball and roller bearing engineering*. SKF Industries, Philadelphia, 3rd edition.

Stammler, M., Schwark, F., Bader, N., Reuter, A. and Poli, G., 2018. "Friction torque of wind-turbine pitch bearings – comparison of experimental results with available models". *Wind Energy*, Vol. 3, pp. 97–105.

Tummala, A. et al., 2016. "A review on small scale wind turbines". *Renewable and Sutainable Energy Reviews*, Vol. 56, pp. 1351-1371.

Vaz, J.R.P., Wood, D.H., Bhattacharjee, D. and Lins, E.F., 2018. "Drivetrain resistance and starting performance of a small wind turbine". *Renewable Energy*, Vol. 117, pp. 509-519.

Wood, D.H., 2011. *Small wind turbines: analysis, design and, application*. Springer, London.

7. RESPONSIBILITY NOTICE

The authors are the only responsible for the printed material included in this paper.